




Study on the effect of the application of metallic alloys on continuous casting machine segment drive roller surface

Jeferson Iorio Tessari ^{1,2*} Matheus Rodrigues Furlani ^{1,2} Henrique Severiano de Jesus ^{1,2} Estéfano Aparecido Vieira ³ 

Abstract

Continuous casting stands as the foremost method for globally solidifying steels. In the context of slab continuous casting machines (CCMs), drive rollers play a pivotal role and are typically forged from steel, with the prevalent use of the EN 42CrMo4 alloy in their manufacturing. However, despite its common usage, this alloy has proved inadequate for resisting severe wear conditions under high temperatures, especially when subjected to contact with the solidified slab (>1000 °C). As a common practice, more wear-resistant steels are used in these rollers through welding techniques, with martensitic ferritic steels frequently utilized for this specific purpose. This study aimed to scrutinize the microstructure and hardness profiles of two rollers subjected to a welding-based coating process, specifically the Submerged Arc Welding. Two ferritic martensitic stainless steels were analyzed. The first steel was a conventional DIN 8555 class UP 5-GF-45-C alloy, characterized by elevated Ni and low Cr content. In contrast, the second a DIN EN 14700 class T Fe8 steel, exhibited higher Mo and lower Ni content. The prepared specimens underwent comprehensive analysis, encompassing measurements of hardness profiles and assessment of microstructural characteristics. The results revealed a decreasing hardness profile close to the base material, exhibiting distinct gradients. Notably, the DIN EN 14700 class T Fe8 steel demonstrates a 33% higher average hardness (Vickers - HV_{0.5}). The material structures were similar, both displaying the typical martensitic morphology. However, in the upper layer of the DIN EN 14700 steel, a microstructure with a relative degradation is observed. The differences in chemical composition caused this effect.

Keywords: Base material; Additive material; Segments; Drive rollers; Submerged Arc Process Welding.

1 Introduction

Continuous casting, a solidification process, shapes molten alloys into forms such as slabs, billets, or preforms. This method is currently the primary choice for solidifying steels, enabling the cost-effective production of items such as slabs and metal with a superior quality. This superiority arises from factors including standardized production, increased production scale, reduced time per ton produced, and the integration of automated systems [1]. These advantages place continuous casting as the predominant process for producing steel products destined for subsequent mechanical forming processes, such as rolling or forging.

Mechanical engineering components frequently experience wear at high operating temperatures, requiring surface treatments to increase their resistance to adverse conditions and achieve the desired performance and service life. In Figure 1, the schematic representation delineates the sections of a continuous slab casting machine, with rolls supporting the slabs during casting exposed to extreme

temperature and mechanical stress conditions. Enhancing the performance of these rollers involves the use of more resilient steel; however, these materials lack mechanical resistance to friction at high temperatures, requiring the application of a coating capable of withstanding these severe conditions. Various techniques, including hot dip, thermal spraying, electroplating, carburizing, gas-phase coating, chemical reduction, and welding, are employed to apply metallic coatings and improve wear resistance [3].

Drive rollers in continuous casting machine segments therefore represent a critical point for the wear of mechanical components. The stress intensity on these rollers varies depending on their position. Notably, at the mold exit, the stress is exceptionally high as the temperature reaches around 1,100 °C when the roller is under casting conditions. Moving down to the intermediate position, despite the slight decrease in temperature, the mechanical effort remains extreme, primarily attributed to the need to bend the slab. At the end of

¹Universidade Federal do Espírito Santo, UFES, Vitória, ES, Brasil.

²ArcelorMittal Tubarão, Serra, ES, Brasil.

³Instituto Federal de Educação Ciência e Tecnologia do Espírito Santo, IFES, Vitória, ES, Brasil.

*Corresponding author: jeferson.tessari@arcelormittal.com.br



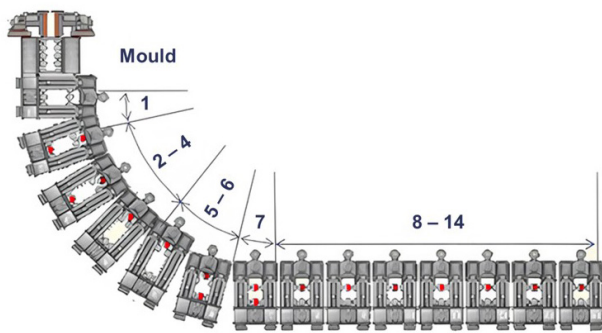


Figure 1. Schematic drawing of a CCM. Adapted from Barcelos and Silva [2].

the line, the rollers experience lower mechanical or thermal stress. As a result, these rollers are susceptible to various environmental factors, such as thermal fatigue caused by high-temperature cycles. Other contributing factors include the mechanical impact from the cast element (slab, billet, or preform) due to their weight and the load resulting from ferrostatic pressure, as well as oxidation and corrosion at high temperatures [4]. In the continuous casting process, the assessment and examination of the rolls to ascertain their remaining service life are imperative.

Throughout steel production, the rolls undergo continual surface wear and thermal fatigue due to the movement of slabs at temperatures ranging from 850 to 1100 °C [5], causing thermal shocks and promoting high-temperature corrosion. The interplay of these factors leads to swift surface deterioration in newly implemented rolls [6,7].

From a tribological perspective, the rollers are submitted to adhesive-abrasive wear. Upon roller and slab contact, adhesive wear with micro-welding occurs. Low-cycle fatigue induces plastic deformation wear, leading to the fatigue failure of the material layers and gradual separation. Additionally, abrasive materials generated or used in the process, such as oxidation residues and caustic products, contribute to roller surface wear [8]. Simultaneously, corrosion pits appear on the roller surface, acting as the initial point for fatigue cracks. This form of stress corrosion primarily occurs in the regions of fatigue cracks under high-temperature load, influenced by the chlorine content in the cooling water [9]. The stress intensity is determined by the thermal gradient and the thermal expansion of the steel in surface layers [10].

It is a widespread practice to manufacture rollers using heat-resistant steels, such as 20Cr13, 25Cr1Mo1V, 40CrMnNiMo, and 24CrMo1V [11,12] alloys. However, a complete roller made from a high-performance wear material only might not always be the most practical solution. Depending on the use, it is typical to design rollers with a material that withstands the mechanical conditions imposed by the machine. Nevertheless, since the surface may not be highly resistant to wear and tear, it is necessary to coat the roller work surfaces with heat-resistant materials. Consequently, enhancing roller surface resistance is a pertinent consideration

in the continuous casting process. One effective method to bolster roller strength involves employing a reconditioning coating. The submerged arc weld coating method is the most common process for coating segment rolls used in the continuous casting process [4]. Thus, in this work, two different coatings were applied to rolls to be used in the first segments of a continuous casting machine for steel slabs, aiming to evaluate the macrostructural variations and the hardness profile reached, thus, defining which one might have better performance.

2 Materials and methods

2.1 Materials

The rolls used in the segment usually comprise three parts, as shown in Figure 2.

Base Material: Generally made from 42CrMo4 EN 10250-3 alloy, forged, quenched, and tempered to a surface hardness of 227-270 HB. For the present study, the focus was on rollers in segments from positions 4 to 6 and 7 to 8, which are subjected to more severe conditions and have a diameter of around 270 mm to 295 mm.

Inner Layer (according to AWS 5.23 EC – F6): it is a transition layer with three functions, with a thickness of 2.0 mm to 2.5 mm, isolating the deposited material from the base, preventing chemical contamination of the coating, creating a gradual transition of the mechanical properties, and preventing the propagation of cracks from the coating to the base.

Coating: The coating is the subject of the present study; it is a layer approximately 3 mm thick created by the SAW process. Two materials were the focus of the study:

- a) **DIN 8555 class UP 5-GF-45-C (conventional):** a metal-cored tubular wire that deposits martensitic stainless steel. This steel has added nitrogen and a lower carbon content. This condition favors the formation of chromium nitrides with a decrease in carbides, promoting resistance to thermal fatigue. Nominal composition according to DIN: C < 0.05%; Si: 0.4%; Mn: 1.00%; Cr: 12%; Ni: 4.2%; N: below 0.5%.
- b) **DIN EN 14700 class T Fe8 (new alloy):** a metal-cored tubular wire. This type of steel generates an oxidation-resistant weld deposit with high hot wear resistance, high tensile strength, and high resistance to metal/metal friction wear. The deposited metal has good hardness retention up to 650 °C and resists scale formation up to 900 °C. This composition also favors resistance to thermal shock and sudden temperature changes. The chemical composition is similar to ASTM – A240 S41500 as follows: C < 0.05%; Mn: 0.5-1.0%; P and S < 0.030%; Si < 0.60%; Cr: 11.5-14.0%; Ni: 3.5-5.5%; Mo: 0.5-1.0%.

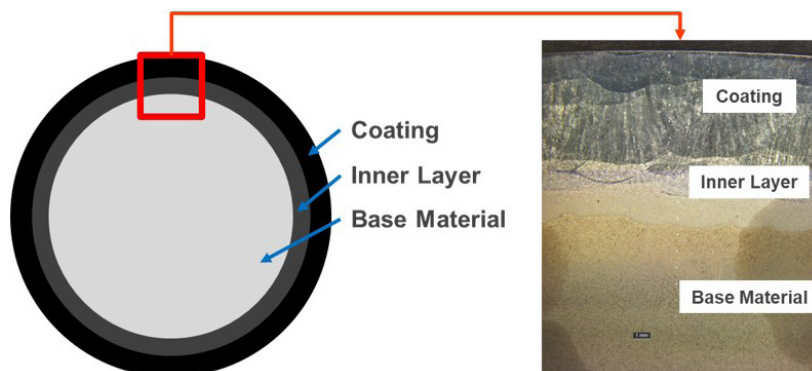


Figure 2. Sample of the manufacturing layout and macrography of the different regions generated in the coating process.

2.2 Welding process

The SAW technique was used to cover the drive rollers, Table 1 presents the main welding parameters.

2.3 Characterization of materials

2.3.1 Metallographic analysis

As explained above, two drive rollers were coated, each with one of the coatings. Table 1 contains the welding conditions. For each condition, a sample of approximately 150 mm × 200 mm × 80 mm, was produced for metallographic analysis and hardness measurements, as seen in Figure 3. There were four positions for the possible fabrication of these samples, arranged at 90° from each other.

2.3.2 Metallographic preparation

After cutting and removing the samples containing the coatings, the metallographic preparation proceeded according to the steps described below:

- Embedding the samples in the BUEHLER SimpliMet 4000 Machine (Bakelite resin; 160 °C temperature and 4200 Psi);
- Sanding of the samples using BUEHLER EcoMet 250 Grinder Polisher with the following sequence of sandpapers: 180, 320, 500, 1200 Mesh.
- Polishing using BUEHLER EcoMet 250 Grinder Polisher with diamond suspension solution (170 RPM and 5 min);
- Chemical etching using Vilella reagent to reveal stainless steel (coating) and 2% Nital to reveal carbon steel microstructure (base material).
- Obtaining micrographs using LEICA DM600 Optical Microscope.
- Obtaining SEM (Scanning Electron Microscopy) images through the JEOL MEV-FEG equipment, 7100-F model.

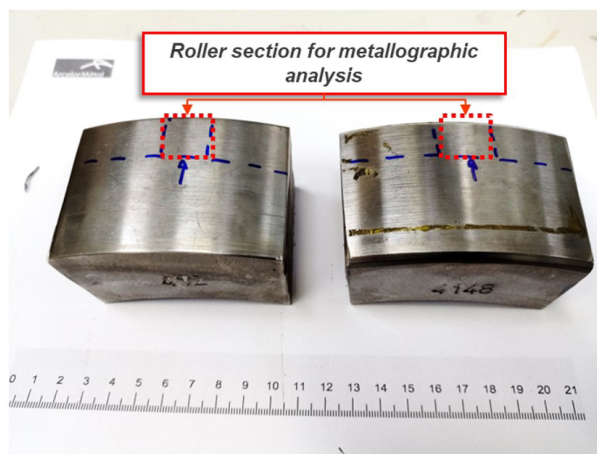


Figure 3. Sectioning of samples for coating evaluation.

Table 1. Welding Parameters

Parameters	Value/Characteristic
Base Material	42CrMo4 EN 10250-3, forged, quenched and tempered, surface hardness 227-270 HB
Welding process	SAW
Deposition technique	Flat position
Filler Metal	DIN EN14700 T Fe8 / DIN 8555 UP 5-GF-45-C
Welding Flux	DIN 32522
Preheating temperature	maximum 300 °C
Welding amperage	> 300 A
Voltage	30 V
Number of layers	maximum 6
Layer thickness	> 0.5 mm
Final hardness expected on the coating	50 HRC

For this study, a stereoscopic macrograph of the sample profile was made, highlighting the different layers formed in the welding process: coating, dilution layer, inner layer, and base metal. Figure 4 schematically shows the reference positions and their depths.

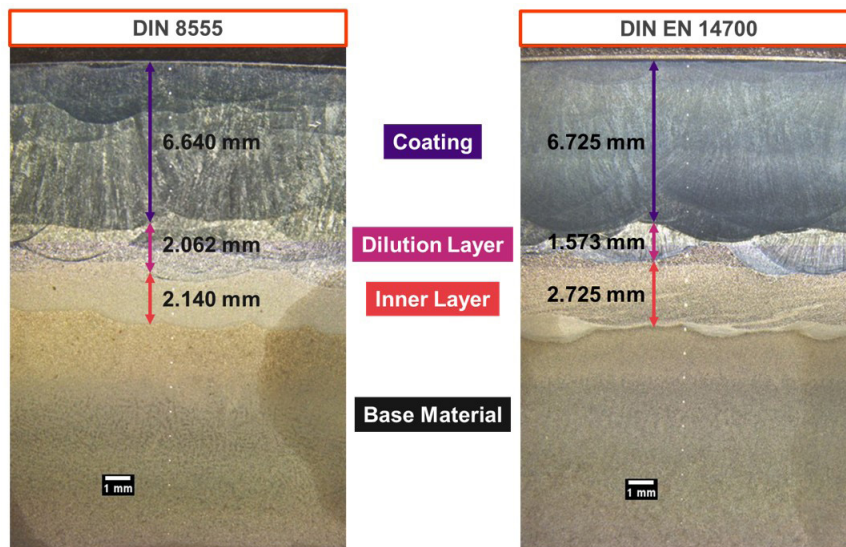


Figure 4. Stereoscope image showing existing layers after the SAW process. Chemical etching: 2% Nital and Vilella. Stereoscope magnification: 7.3x.

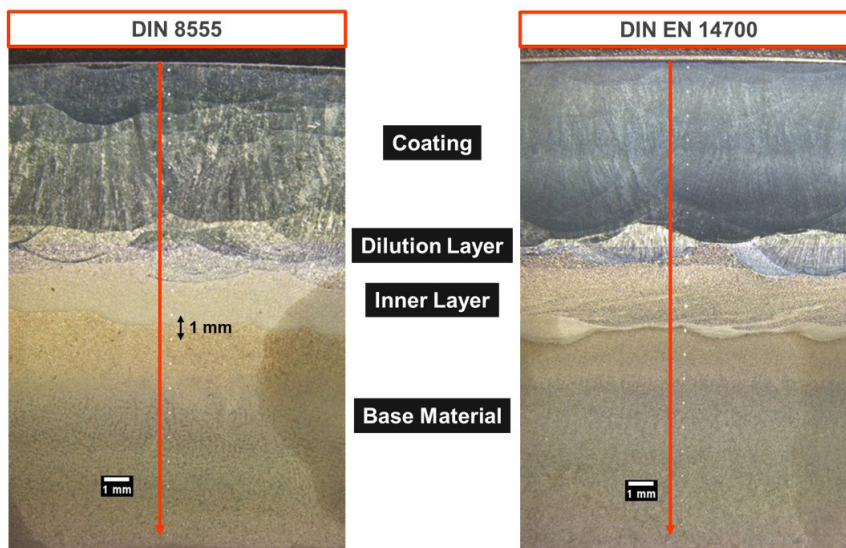


Figure 5. Sequence of hardness measurements made along the different materials. Chemical etching: 2% Nital and Vilella. Stereoscope magnification: 7.3x.

2.4 Hardness tests

The ZWICK ZHU microhardness tester was used for the Vickers hardness test. The load applied was 500gf or 0.5kgf. The hardness was measured at a spacing of 1,000 micrometers. Figure 5 schematically illustrates the positions of the indentations made from 0 to 20 mm.

3 Results and discussion

3.1 Microstructure

Figure 6 and Figure 7 shows coating microstructure for DIN 8555 and DIN EN 14700 respectively. Also, it is presented the microstructure for the dilution layer, inner

layer and base material for both roller-experiment after a chemical attack with Vilella. For the DIN 8555 steel coating (conventional alloy) a structure composed of lath martensite is observed on the surface, suggesting high hardness. The rather refined structure probably contains ferrite and pearlite.

In the case of the DIN EN 14700 steel illustrated in Figure 7, chemical etching of the surface region (coating) makes visible the dendritic microstructure of the weld deposit without revealing much about the constituents. The dilution layer region shows the presence of lath martensite, and the base material displays a structure that incorporates both ferrite and pearlite. However, compared to the base material shown in Figure 6, a clearly defined and coarser microstructure is apparent, characterized by an increased presence of pearlite.

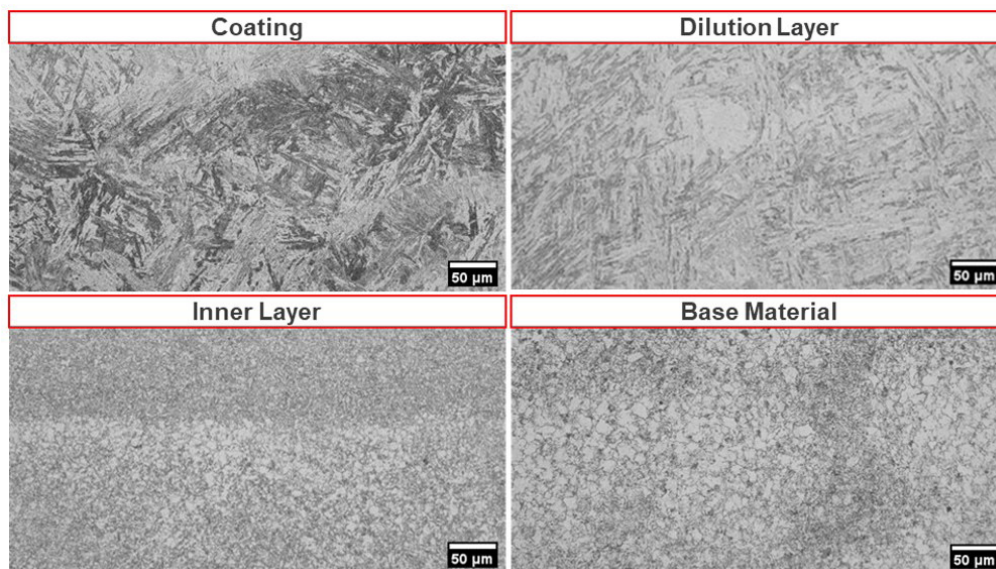


Figure 6. Optical microscope image showing the microstructures formed in the DIN 8555 welding process. Chemical etching: 2% Nital and Vilella. Optical microscope magnification: 200x.

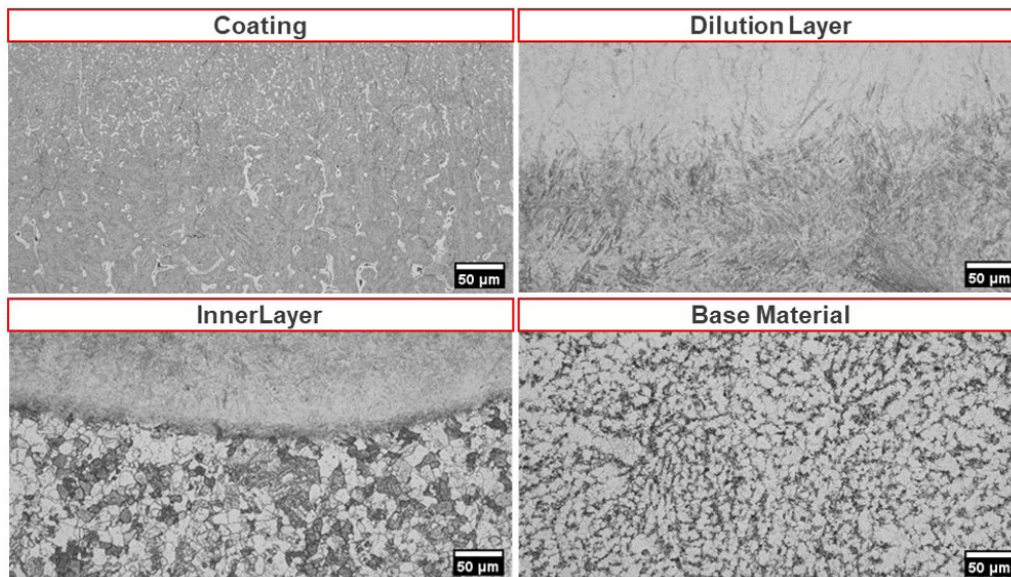


Figure 7. Optical microscope image showing the microstructures formed in the DIN EN 14700 welding process. Chemical attack: 2% Nital and Vilella. Optical microscope magnification: 200x.

The microstructure and its contours are better defined in the DIN EN 14700 material, as opposed to the DIN 8555 material, which exhibits the presence of a metastable and dense microstructure.

The results in Figure 7 show that the new alloy (DIN EN 14700) has a microstructure similar to dendrites, however, in the intermediate region, there are probable signs of formation of lathed martensite, not observed in the DIN 8555 material.

Figure 8 compares the microstructure obtained by SEM in the cladding region, and can observe the lath martensite in more detail. These laths, which previously could not be identified in Figure 7, have now been revealed for the

DIN EN 14700 (new alloy) material with a microstructure containing the laths, but in a much more refined way. The second phase observed, probably is characterized as delta ferrite. Perhaps, refined microstructure and differences in chemical composition may explain a potential behavior of greater hardness in this material [10].

Figure 9 illustrates that the post-coating process of both materials produced a metal microstructure primarily composed of ferrite and cementite. Nevertheless, the material coated with DIN 14700 exhibits a more refined microstructure. Discrepancies can be deduced from the respective contributions and thermal conductivities of each alloy generated during the coating process.

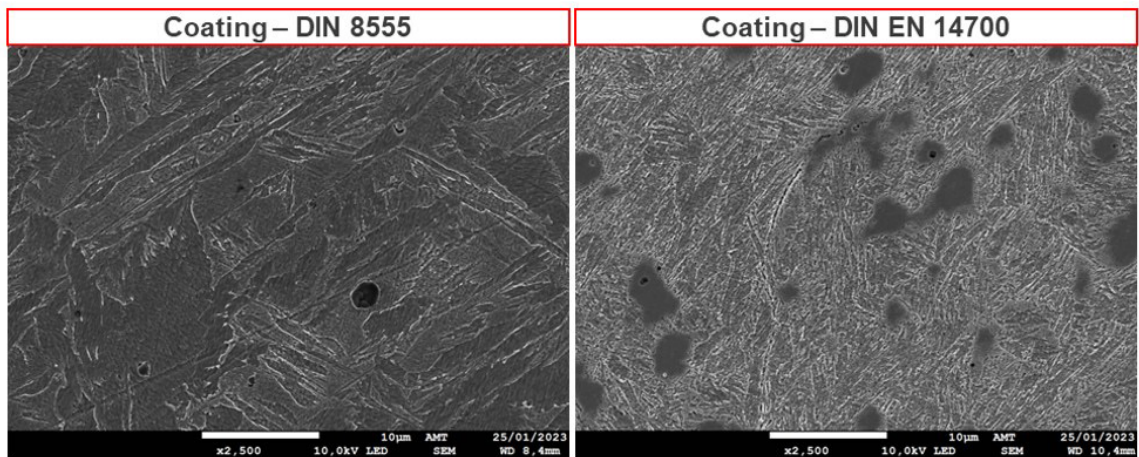


Figure 8. Coating analyzed via SEM after the Vilella attack. SEM magnification: 2500x

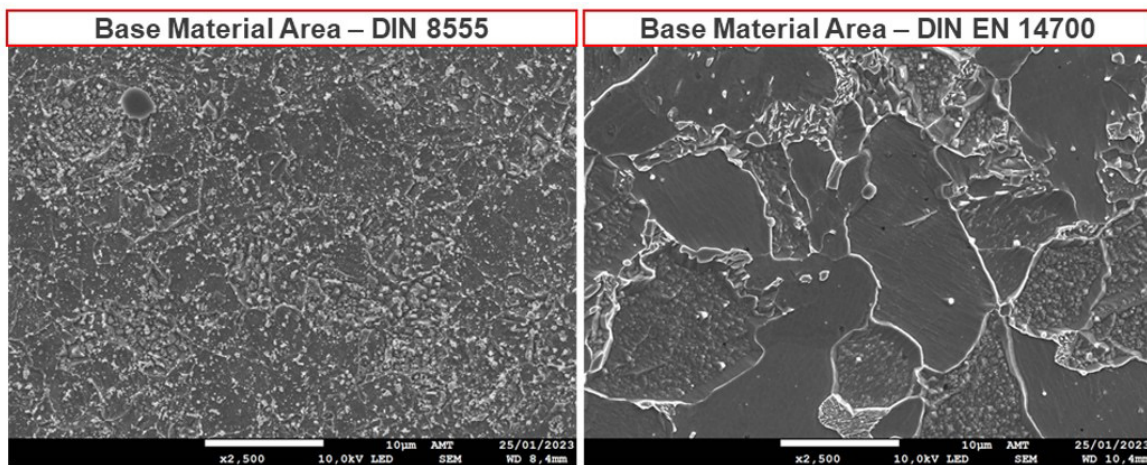


Figure 9. Base material analyzed via SEM after the 2% Nital attack. SEM magnification: 2500x.

Due to the distinct chemical compositions of the alloys, they will inherently exhibit different Time-Temperature-Transformation (TTT) curves. As reported by Mariano et al. [13] in a study of similar steels containing 2 to 6% Ni, it was expected that the DIN 8555 alloy would have its curves shifted more to the left due to its lower Ni percentage in the composition.

This observation is confirmed by the macrographic images in Figure 4, which reveal a sequential execution of the welding process with possible variations in the thermal inputs and deposited material ranges between stages. Notably, the transition zone between the base material and the additional material shows a depth variation of approximately 2 mm, indicating a more extensive thermally affected area in the DIN EN 14700 standard material.

3.2 Hardness

Figure 10 shows the hardness data. The comparison reveals that the average surface hardness of the new material is 33% higher than that of the material currently used. Additionally, there is a more gradual transition in hardness between the coating and the base metal for DIN 8555, a

feature not observed in the new material. The initial decline in hardness for both materials occurs during the formation of the inner layer. The subsequent evolution of hardness is influenced by the distinct characteristics inherent to each material and the application procedure.

Notably, this reduction in hardness has implications for the material's susceptibility to embrittlement, particularly when the wear depth reaches approximately 9 mm for the new alloy and 15 mm for the traditional alloy.

4 Measurements on the CCM

For this study, hardness assessments were conducted on a continuous casting machine at segment 8, as outlined in Figure 1. The rationale behind this selection stems from its unique position after the bend in the horizontal segment of the machine, marking the start of the straight portion with a single drive roller. This segment assumes greater significance due to its pivotal role in the final unfolding of the steel slab along the shaft, consequently avoiding the calendaring effect. Notably, during this phase, the slab is oriented horizontally, causing substantial mechanical loads on the drive roller of

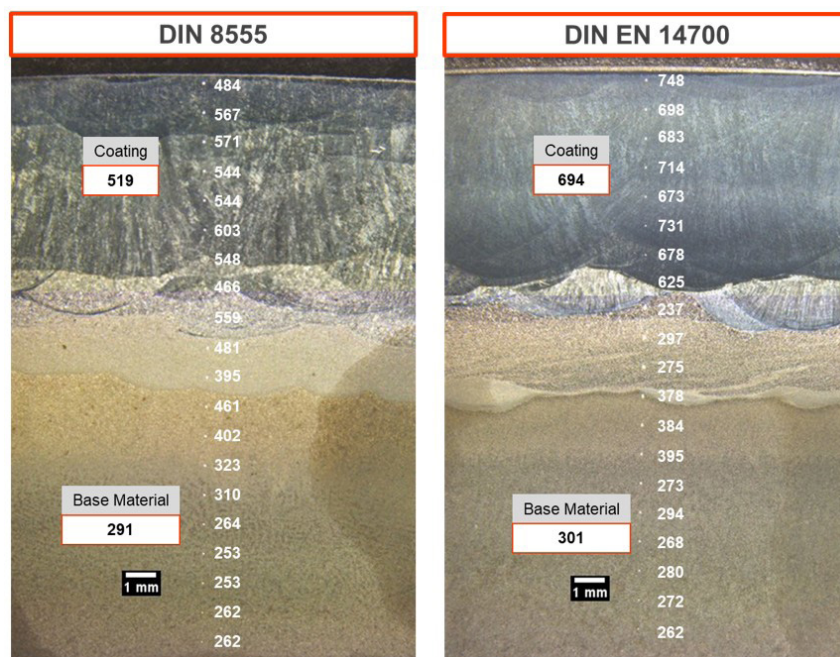


Figure 10. Vickers hardness of DIN 8555 and DIN EN 14700 coatings.

Table 2. HRC hardness measured in the drive roller of segment 8 present in CCM #1

Coating	Measurement date	Production [t]	Diameter [mm]		Hardness [HRC]	
			Initial	Obtained average	Initial	Obtained average
DIN 8555	11/14/2023	695,485	295.00	294.89	45 ~ 48	45.37
DIN 14700	11/14/2023	554,745	295.00	294.69	45 ~ 49	46.12

this specific segment, as illustrated schematically in Figure 1. To comprehensively capture the hardness characteristics, measurements were conducted across the upper section at six predetermined and equidistant locations, maximizing the scope of observation scope throughout the continuous casting process.

Table 2 displays the initial measurements obtained. The hardness achieved for both materials remains stable after the production of 695,485 tons for the DIN 8555 material and 554,745 tons for the roll coated with the new DIN EN 14700 alloy. These values are promising, although they depend on an extended operational time of the rolls for definitive evaluations.

5 Conclusions

The results obtained in the laboratory after the tests show that the metallographic characteristics of the materials have structures containing lath martensite. However, the new material has a more refined lath formation. We also observed the presence of delta ferrite in the midst of a high-strength constituent. Despite the presence of inclusions in both materials, the similarity indicates that the change in mechanical properties will be equally equivalent and of low deleterious effect.

The information obtained in the tests and based on the follow-up of measurements in the field, indicate that the new alloy can present greater mechanical resistance in hot work for the positions of the segments mounted on a machine shaft (segment 4/6 and segment 7/8) of 14 segments per strand, however, due to the sharp transition zone observed in the optical micrograph, a rapid drop in hardness of the new alloy compared to the current material is expected when approaching surface wear above 1 mm in the roll radius. However, the high hardness of the new alloy, in theory, can increase the material’s resistance to wear, which would be beneficial to increasing the service life of the roller.

Acknowledgements

This work was supported by ArcelorMittal Tubarão and IFES – state of Espírito Santo Federal Institute. Authors are grateful to the Brazilian government agencies for research development: FAPES – Research Support Foundation - ES-Brazil, CNPq – National Council for Scientific and Technological Development, Capes – High Education Personnel Improvement Coordination, and FINEP – Studies and Projects Financier for their collaboration.

References

- 1 Vynnycky M. Continuous casting. *Metals*. 2019;9(6):643.
- 2 Barcelos GC, Silva LC. Estudo dos registros de manutenção de segmentos das máquinas de lingotamento contínuo da CST [monograph]. Vitória: Universidade Federal do Espírito Santo; 2005.
- 3 Gentil V. Corrosão. 5ª ed. Rio de Janeiro: LTC; 2007.
- 4 Makarov AV, Kudryashov AE, Nevezhin SV, Gerasimov AS, Vladimirov AA. Reconditioning of continuous casting machine rollers by laser cladding. *Journal of Physics: Conference Series*. 2020;1679(4):042047-7.
- 5 Schwerdtfeger KJ. Heat withdrawal in continuous casting of steel. In: Cramb AW, editor. *The making, shaping and treating of steel: casting volume*. 11th ed. Pittsburgh: AISE Steel Foundation; 2003. p. 1-41.
- 6 Bhattacharya AK, Sambasivam D. Optimization of oscillation parameters in continuous casting process of steel manufacturing: genetic algorithms versus differential evolution. In: Santos WP, editor. *Evolutionary computation*. London: IntechOpen; 2009. p. 77-102.
- 7 Mazumdar S, Ray SK. Solidification control in continuous casting of steel. *Sadhana*. 2001;26(1-2):179-198.
- 8 Viňáš J, Brezinová J, Guzanová A. Analysis of the quality renovated continuous steel casting roller. *Sadhana*. 2013;38(3):477-490.
- 9 Blaškovič P, Čomaj M. Renovation by cladding and thermal spraying. Bratislava: STU Bratislava; 2006. 204 p.
- 10 Kasala J, Pernis R, Mäsiar H. An application of robust parameter design using Taguchi method. In: *Proceedings of the 9th International Foundrymen Conference*; 2009 June 18-19; Zagreb. Sisak: Faculty of Metallurgy, University of Zagreb; 2009.
- 11 Kirchu IF, Stepanova TV, Suprun MV. Experience of using rollers made of 25Cr2Mg1AV steel on a slab continuous casting machine. *Steel*. 2015;1:68-72.
- 12 Mei PR. Aços e ligas especiais. 3ª ed. São Paulo: Blucher; 2010.
- 13 Mariano NA, Pereira VF, Rodrigues CAD, di Lorenzo PL, Rollo JMDA. Caracterização da temperabilidade e das curvas de transformação de fases de aços inoxidáveis martensíticos do tipo FeCrNi. *Revista Escola de Minas*. 2007;60(1):163-167.

Received: 12 Sept. 2023

Accepted: 22 July 2024